A Parametric Study of the Bouc-Wen Model for Bolted Joint Dynamics

Drithi Shetty*

Postdoctoral Associate
Department of Mechanical Engineering
Rice University
Houston, Texas 77005
Email: drithi.shetty@rice.edu

Matthew Allen

Professor
Department of Mechanical Engineering
Brigham Young University
Provo, Utah 84602
Email: matt.allen@byu.edu

Built-up structures exhibit nonlinear dynamic phenomena due to friction at the surfaces that are held together using mechanical fasteners. This nonlinearity is hysteretic, or history dependent. Additionally, interfacial slip results in stiffness and damping variations that are dependent on the vibration amplitude. In the microslip regime, the dissipation varies as a power of the amplitude. The four-parameter Iwan model can capture both the hysteretic and power-law dissipation behavior that is characteristic of many bolted joints. However, simulating the dynamic response of this model is computationally expensive since the states of several slider elements must be tracked implicitly, necessitating the use of fixed-step integration schemes with small time steps. The Bouc-Wen model is an alternative hysteretic model in which the restoring force is given by a first order nonlinear differential equation. Numerical integration of this model is much faster because it consists of just one additional state variable, i.e. the hysteretic variable. Existing literature predominantly focuses on studying the steady-state behavior of this model. This paper tests the effectiveness of the Bouc-Wen model in capturing power-law dissipation by comparing it to four-parameter Iwan models with various parameters. Additionally, the effect of each Bouc-Wen parameter on the overall amplitude-dependent damping is presented. The results show that the Bouc-Wen model cannot capture power-law behavior over the entire microslip regime, but it can be tuned to simulate the response over a smaller amplitude range.

*Address all correspondence to this author.

1 INTRODUCTION

Mechanical fasteners are commonly used to assemble various parts in built-up structures, making manufacturing and maintenance of these structures convenient. These fasteners have a nonlinear effect on the overall stiffness and damping of the structure due to frictional energy losses at the interface [1, 2]. The contact pressure at the interface due to bolt preload is non-uniform, with the pressure being high near the bolt hole and gradually decreasing further away [3]. As a result, at low tangential loads, the area near the bolt hole remains stuck whereas the edges of the contact interface start to slip. This phenomenon is termed microslip. The area that remains stuck can be understood to behave like a linear spring, whereas the area that slips results in frictional energy dissipation and a loss of stiffness [4]. Various experimental studies have found that, so long as the joint doesn't slip completely, the stiffness of the joint tends to decrease slightly while the damping increases significantly, potentially by orders of magnitude [5–7]. The nonlinear resonant frequency and dissipation can be quantified as a function of the amplitude. For bolted joints, the dissipation is found to vary as a power of the load amplitude [8, 9], so that the log of the damping is a linear function of the log of the vibration amplitude. This is referred to as power-law behavior. If the force amplitude increases further, the area of contact reduces, ultimately resulting in relative motion between the surfaces, also known as macroslip. In macroslip, the joint stiffness decreases significantly and the dissipation exhibits power-law behavior with a different exponent (or slope). Additionally, due to interfacial slip, the stress-strain, or force-displacement relationship is hysteretic in nature, i.e. the restoring force depends not

only on the displacement but also on the past state of the system.

One approach to simulate the dynamics of jointed structures could be to create a high-fidelity finite element (FE) model of the bolted structure that is able to capture the dissipation due to friction in the microslip and macroslip regime [10, 11]. However, due to the orders-of-magnitude difference in the length scales associated with microslip and that of the whole model, this approach is highly computationally expensive [12]. Jewell et al. [11] observed that a fine mesh is needed around the contact region to effectively capture microslip nonlinearity, especially at low displacement amplitudes. An alternative is to replace the contact interface with a constitutive model capable of simulating the hysteretic and amplitude-dependent nonlinear behavior that has been observed experimentally. The constitutive model could then be incorporated into the FE model using whole-joint modeling [9] or similar approaches. In the whole-joint approach, the nodes on a contact surface are constrained to a single virtual node. The appropriate hysteretic model is then applied between the virtual nodes of the surfaces in contact. While this approach is computationally more efficient than creating a high-fidelity FE model, it is difficult to isolate the effect of each joint on the overall system dynamics. Therefore, computationally intensive optimization schemes are required to calibrate the constitutive models [13]. Alternatively, a modal modeling approach can be used [14], in which each mode is represented by a single degree-of-freedom (SDOF) system with a parallel arrangement of a linear spring, linear damper and the hysteretic model.

In either of the modeling approaches, a suitable constitutive model is required to capture the nonlinear dynamics of the bolted joint(s). Gaul and Nitsche [15] reviewed different models that can be used to estimate the dynamics due to bolted joints. More recently, Mathis et al. [16] presented an overview of various rate-dependent and rate-independent hysteretic models. One such model prevalent in bolted joint dynamic analysis is the Iwan model [17]. It consists of a parallel arrangement of spring-slider units, known as Jenkins elements, with all elements having the same spring stiffness but different slider strengths. A distribution function is defined to specify the strength of the sliders. Several forms of the Iwan model have been developed for bolted joints applications [18–20]. Among them, Segalman's four-parameter Iwan model [19] is most popular since it can capture the microslip power-law dissipation behavior that has been experimentally observed. However, an implicit integration scheme is required to simulate the dynamic behavior of the Iwan model, with the state of the sliders being evaluated sequentially at each time step. The speed of numerical computation depends on the number of sliders, or discrete elements that define the distribution function. Typically, $30-100$ sliders are used, resulting in high computational cost. Brake [21] presented a reduced formulation of the four-parameter model that makes it possible to derive an analytical expression for the nonlinear force, thus circumventing the slider state calculations. Alternatively, Shetty and Allen [22] used closed-form expressions for stiffness and dissipation to reformulate the differential equations of the four-parameter model such that explicit ODE solvers can be used. However, the closed-form expressions used are applicable only in the microslip regime.

The Bouc-Wen model [23, 24] is another semi-physical, rate-independent model that can capture hysteretic behavior. It consists of a nonlinear, first-order ordinary differential equation (ODE) that relates the input displacement to the output restoring force in a hysteretic way. The equation of motion for this model can be written in state-space form. Therefore, it can be integrated using explicit ODE solvers such as the Runge-Kutta method [25]. Since the hysteretic variable defined by the nonlinear ODE is the only additional state variable, dynamic simulation of the Bouc-Wen model is more computationally efficient than the four-parameter Iwan model. The Bouc-Wen model is regarded as semi-physical since its formulation is based on some physical understanding of hysteresis but its parameters are non-physical. Ismail et al. [26] provide an extensive survey of the Bouc-Wen model.

A vast majority of the existing literature focuses on applying the Bouc-Wen model to capture steady-state hysteretic behavior of various nonlinear systems [27–29]. There has been some effort to simulate the hysteretic behavior due to friction using this model [30, 31]. Allen et al. [32] observed good agreement between the time responses of a reduced-order model with nonlinearity represented using the Bouc-Wen formulation and a detailed FE model of a complex, large-scale aerospace structure with stick-slip elements in many joints. However, to completely characterize the nonlinearity in a bolted structure, the frequency and power-law damping behavior over a range of vibration amplitude must be considered. Porter et al. [33] took a step towards this, assessing the ability of several hysteretic models (including the Bouc-Wen model) to fit experimental frequency and damping curves by using multi-objective optimization to identify the parameters. This paper seeks to shed further light on this issue, focusing on characterizing the ability of the Bouc-Wen model to capture the microslip-level power-law dissipation behavior that is characteristic of bolted joint dy-

namics. The effect of each Bouc-Wen parameter on the overall damping behavior is also studied.

The following section provides background on the four-parameter Iwan model, the Bouc-Wen model and the modal modeling approach. A method to identify the Bouc-Wen model parameters from quasi-static force-displacement data is also included. Section 3 compares the dynamic response of the two hysteretic models to an impulsive force, analyzing the Bouc-Wen model's effectiveness in simulating power-law dissipation behavior. Section 4 provides an analysis of the effect of each Bouc-Wen parameter on the overall damping of the system. Finally, the conclusions are presented in Sec. 5.

2 BACKGROUND

2.1 The Four-Parameter Iwan Model

The Iwan model [17] is a lumped, hysteretic model that was originally developed to characterize metal elasto-plasticity. It consists of a parallel arrangement of spring-slider units, also known as Jenkins elements. The nonlinear restoring force due to the Iwan model is given by Eq. 1,

$$f_{\mathrm{nl,Iwan}}(x,t,\phi) = \int_0^\infty \rho(\phi)[x(t) - u(t,\phi)]d\phi \qquad (1)$$

where $x(t)$ is the imposed displacement, $u(t,\phi)$ is the displacement of the Jenkins elements that constitute the Iwan model, and $\rho(\phi)$ is the density of sliders that have strength ϕ. Thus, the formulation of $\rho(\phi)$, also referred to as the distribution function, defines the slip behavior of the Iwan model. Note that, for an SDOF system, $x(t)$ is the displacement of the mass whereas for an MDOF system, it is the difference between the displacements of nodes that are connected with the Iwan element. The dissipation due to bolted joints in the microslip regime exhibits power-law behavior [8, 9], i.e. the dissipation increases with some power of the the applied load amplitude. Segalman [19] defined a distribution function for the Iwan model that is able to capture this power-law behavior. The resulting model is referred to as the four-parameter Iwan model, and its distribution function can be written as

$$\rho(\phi) = R\phi^{\chi}[\mathrm{H}(\phi) - \mathrm{H}(\phi - \phi_{\max})] + S\delta(\phi - \phi_{\max}), \quad (2)$$

where $H(.)$ and $\delta(.)$ are Heaviside and Dirac-delta functions respectively. This model form can thus be represented by the parameter set $[\phi_{\max}, \chi, R, S]$,where $\phi_{\max}$ is the displacement at which all sliders slip (i.e. macroslip occurs), χ is a dimensionless quantity that governs the slope of the power-law energy dissipation versus amplitude, and R and S can be understood as the stiffness of the power-law portion of the distribution and the delta function portion of the distribution respectively. Since the parameters R and S do not have physically meaningful units, Segalman proposed using another set of more intuitive parameters, $[F_{\mathrm{S}}, K_{\mathrm{T}}, \chi, \beta]$, with F_{S} being the force required to cause macroslip, K_{T} being the tangential stiffness of the joint at small applied loads, and χ and β being dimensionless parameters.

In order to simulate the nonlinear force due to the Iwan model using numerical methods, Eqs. 1 and 2 must be written in discrete form with a finite number of discretization points. Typically, $30 - 100$ discretization points are sufficient, depending on the range of amplitude being simulated. Equation 1 in discrete form is composed of a summation of the friction forces due to the sliders that have slipped and the linear spring forces due to the sliders that remain stuck. Thus, the density of sliders that have slipped and that are stuck must be evaluated, resulting in $30 - 100$ additional state variables in the nonlinear equation. It is computationally expensive to simulate the dynamic response of the Iwan model because the state of all sliders needs to be evaluated at each time step. Additionally, the slider positions depend on their prior state and on the displacement. Thus, one must iterate to find their states at each time step; i.e. the equation of motion cannot be cast in the form $\dot{\mathbf{y}} = f(\mathbf{y}, t)$ that is required for most ODE solvers. Further details about the model formulation and discretization procedure can be found in [9].

2.2 The Bouc-Wen Model

Another model that can capture hysteretic behavior is the Bouc-Wen model [23, 24]. This formulation is intended for any form of hysteresis and was originally applied to force – deflection and flux– current diagrams of mechanical and ferromagnetic hysteresis. In case of the Bouc-Wen model, the nonlinear restoring force is given as

$$f_{\mathrm{nl,BW}}(x,z) = (1-\alpha)K_0 z \qquad (3)$$

where K_0 is the initial low-amplitude stiffness and α is defined as the ratio of macroslip stiffness to initial stiffness. The hysteretic state variable, $z(t)$ is defined by the following ODE,

$$\dot{z} = A\dot{x} - \beta|\dot{x}||z|^{n-1}z - \gamma\dot{x}|z|^n \qquad (4)$$

where A, β, γ and n are the Bouc-Wen parameters that can be tuned to fit force-displacement data obtained either experimentally or using FE simulations. Thus, the hysteretic variable z is an additional state variable to be solved for, along with the displacement and velocity, when computing the dynamic response of a system consisting of a Bouc-Wen model. However, this is just one additional variable as opposed to the state of all sliders in the Iwan model resulting in the addition of $30-100$ state variables. Therefore, this formulation provides a computational advantage over the four-parameter Iwan model. Additionally, the system of ODEs takes the form $\dot{\mathbf{y}} = f(\mathbf{y}, t)$ where y is the vector of state variables. Thus, the ODEs can be solved using explicit solvers like the Runge-Kutta methods. For $n = [1, 2]$, closed-form solutions for z can be obtained [34], but other values of n, including non-integer values, are often needed to obtain the desired behavior. In the context of structural dynamics, the Bouc-Wen model is considered semi-physical in nature since, unlike the spring-slider units in Iwan models, the state variable $z(t)$ does not have a specific physical interpretation. Note that Guo et al. [35] proposed an equivalent normalized Bouc-Wen model with parameters that can be qualitatively linked to the shape of the hysteresis curve.

2.3 Identifying the Parameters of the Bouc-Wen Model

An adaptation of the identification method presented in [36] has been used to identify Bouc-Wen parameters for a given load-displacement hysteresis loop. Consider an SDOF system with hysteretic nonlinearity that is being reproduced using the Bouc-Wen model. The equations for the Bouc-Wen formulation are given by Eq. 3,4. The parameter α is given as the ratio of K_∞, the linear stiffness in the macroslip regime with respect to K_0, the linear stiffness at low amplitudes, i.e. before slip occurs. If the low-amplitude linear natural frequency, ω_0, and the high-amplitude slip frequency, ω_∞, of the system are known instead, the corresponding linear stiffness can be calculated as a square of the natural frequency. Thus, α can be calculated using the relation

$$\alpha = \left(\frac{K_\infty}{K_0}\right) = \left(\frac{\omega_\infty}{\omega_0}\right)^2. \tag{5}$$

Since the parameter A is the coefficient of the linear term in Eq. 4, it can be set to unity if the estimate of stiffness using the low-amplitude linear frequency is expected to be accurate. Next, eliminating the time dependence and switching from differential in Eq. 4 to difference gives

$$\triangle z = \triangle x - \beta|\triangle x||z|^{n-1}z - \gamma\triangle x|z|^n. \tag{6}$$

Suppose the hysteresis of the system has been measured, collecting the displacements of the system in the vector $\mathbf{x}$ and the corresponding restoring forces in $\mathbf{f}_{\text{nl}}$. These could be plotted to view the hysteresis loop that the system would exhibit in steady-state oscillation. The hysteretic variable z can be calculated from the nonlinear force and displacement vectors, i.e. $\mathbf{f}_{\text{nl}}$ and $\mathbf{x}$ respectively, using Eq. 7, obtained by re-arranging Eq. 3.

$$\mathbf{z} = \frac{1}{(1-\alpha)K_0}\mathbf{f}_{\text{nl}} \tag{7}$$

Note that $\mathbf{z}$ in Eq. 7 is a vector, giving the value of the hysteretic variable for every value of $\mathbf{f}_{\text{nl}}$. Therefore,

$$\triangle\mathbf{z} = \frac{1}{(1-\alpha)K_0}\triangle\mathbf{f}_{\text{nl}} \tag{8}$$

where $\triangle\mathbf{f}_{\text{nl}}$ is the difference between consecutive values of the vector $\triangle\mathbf{f}_{\text{nl}}$. Substituting Eq. 8 in Eq. 6 gives

$$\frac{\triangle\mathbf{f}_{\text{nl}}}{(1-\alpha)K_0} - \triangle\mathbf{x} = \left[-\triangle\mathbf{x}|\mathbf{z}|^{n-1}\mathbf{z} \; -\triangle\mathbf{x}|\mathbf{z}|^n\right]\begin{bmatrix}\beta\\ \gamma\end{bmatrix}. \tag{9}$$

Equation 9 is of the form $\mathbf{Y} = \mathbf{\Phi\Theta}$ which can be solved for $\mathbf{\Theta}$ by taking the pseudo-inverse of $\mathbf{\Phi}$, for a constant value of n. To ensure that the matrix $\mathbf{\Phi}$ is well-conditioned, each column of $\mathbf{\Phi}$ is normalized to its corresponding maximum value. In order to obtain an optimal set of parameters $[n, \beta, \gamma]$, the least-squares regression problem, given by Eq. 9, is solved iteratively for different values of n, and the parameter set that results in the lowest error is used. Although the method presented in [36] considered n to be constant, it has been varied in this study since n impacts the amplitude-dependent dynamic behavior of the Bouc-Wen model, as will be discussed in Sec. 3.2. Note that this method can also be applied to a single mode of a nonlinear system when using the modal modeling approach, described below. In this case, x is replaced by the modal displacement q.

2.4 Modal Modeling Approach

Consider the FE model of a structure where each bolted joint is represented by a constitutive model. The

resulting equation of motion (EoM) is given by Eq. 10,

$$\mathbf{M}\ddot{\mathbf{x}} + \mathbf{C}\dot{\mathbf{x}} + \mathbf{K}_\infty \mathbf{x} + \mathbf{f}_{\text{nl}}(\mathbf{x}, h) = \mathbf{f}_{\text{ext}}(t) \tag{10}$$

where $\mathbf{M}$ is the mass matrix, $\mathbf{C}$ is the linear damping matrix, $\mathbf{K}_\infty$ is the linear stiffness matrix if all the joints were disconnected, and $\mathbf{f}_{\text{nl}}(\mathbf{x}, h)$ is the vector of nonlinear joint forces given by a hysteretic model, that depend on the nodal displacements $\mathbf{x}$ and the hysteretic state h. The hysteretic state is simply the variable z for the Bouc-Wen model, while for an Iwan model it is a vector of slider states $\boldsymbol{\phi}$. As discussed earlier, it is difficult to isolate the effect of each joint on the overall system dynamics, so it is non-trivial to use Eq. 10 to calibrate the parameters of the hysteretic models to match measurements.

As an alternative, Segalman [14] proposed a modal modeling approach, where each nonlinear mode of the structure is represented by a single degree-of-freedom (SDOF) system with a parallel arrangement of a linear spring, linear damper and a nonlinear hysteretic element. This approach makes two important assumptions. Firstly, it assumes that there is no coupling, or energy transfer, between the modes. This assumption holds true if the external force results in excitation of a single, dominant mode. Eriten et al. [37] showed that in a weakly nonlinear structure, the interaction between modes is not significant if their natural frequencies, or harmonics of the frequencies, are sufficiently spaced. On the other hand, Moldenhauer et al. [38] and Wall et al. [39] showed the presence of modal coupling in two different jointed structures. The second assumption is that the low-amplitude, linear mode shapes of the system are preserved and hence applicable in the amplitude range being analyzed. This assumption is often reasonable, as the joints introduce only a weak stiffness nonlinearity and tend to change the global mode shapes relatively little.

While there are limitations to the applicability of the modal modeling method, when the modes do not exhibit coupling this method has proven simple to use and has very accurately captured the observed behavior [7]. As a result, in this paper a modal model is used as a truth model for a system that did not exhibit significant modal coupling. Equation 10 is transformed to the modal domain using $\mathbf{x} = \boldsymbol{\Phi}_0 \mathbf{q}$, where $\boldsymbol{\Phi}_0$ is the low-amplitude, linear mode shape matrix and $\mathbf{q}$ is the vector of modal displacements. If there is no modal coupling, the modal transformation results in the nonlinear joint force $\mathbf{f}_{\text{nl}}$ being projected onto each mode and being a function of the corresponding modal displacement, i.e. $\boldsymbol{\Phi}_{0r}^T \mathbf{f}_{\text{nl}}(\mathbf{x}, h) = \hat{f}_{\text{nl}}(q_r, \hat{h})$, where the $\hat{}$ symbol denotes joint parameters that are defined on a modal basis rather than for actual physical joints. As a result, Eq. 10 reduces to

$$\ddot{q}_r + 2\zeta_{0r}\omega_{0r}\dot{q} + \omega_{\infty r}^2 q + \hat{f}_{\text{nl}}(q_r, \hat{h}) = \boldsymbol{\Phi}_{0r}^T \mathbf{f}_{\text{ext}} \tag{11}$$

for the r^{th} mode. Here, ω_{0r} is the linear frequency of the r^{th} mode at low amplitudes, when there is no slip occurring, whereas $\omega_{\infty r}$ is the frequency at macroslip. It is also assumed that the modal transformation results in a diagonal linear damping matrix, with ζ_{0r} being the low-amplitude damping ratio of the r^{th} mode. Each nonlinear mode can be independently analyzed using a suitable hysteretic model to represent the modal joint force, $\hat{f}_{\text{nl}}(q_r, \hat{h})$. Figure 1 provides a schematic of the modal model.

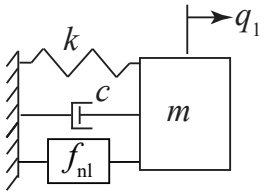

Fig. 1: Modal model: SDOF system with a linear spring, damper and nonlinear element in parallel. In this work $m = 1$, $k = \omega_\infty^2$, $c = 2\zeta_0\omega_0$ and $\hat{f}_{\text{nl}}$ is the force defined by either a Bouc-Wen or Iwan element.

Modal models significantly reduce the computation cost of dynamic simulations. Deaner et al. [6] and Roettgen and Allen [7] showed that the modal Iwan model is capable of describing the nonlinearity in various bolted structures. Further, Lacayo et al. [40] found that this approach can accurately capture the nonlinear response to an impulse-type excitation (that excites different modes of the structure to varying extents) if it consists of one dominant mode, and may still be fairly acceptable in cases of more than one dominant mode, provided the mode being studied is a dominant one. This paper evaluates the effectiveness of the Bouc-Wen model as a modal model, in terms of its ability to capture the nonlinear behavior that has been observed experimentally for a mode of a specific structure. In the authors' experience, the behavior chosen is typical of that of many structures with bolted interfaces.

3 COMPARING THE BOUC-WEN AND IWAN MODELS

An assembly of two beams bolted together, commonly referred to as the Sumali beam, was used to evaluate the capability of the Bouc-Wen model and to compare it to that of the four-parameter Iwan model. The structure, as seen in Fig. 2a, consists of two thin, identical, stainless steel beams of length 508 mm, width 50.8 mm, and thickness 6.35 mm, that overlap and are joined with four bolts. Deaner et al. [6] experimentally analyzed the first three elastic modes of this structure and fit suitable modal Iwan models to capture the observed amplitude-dependent behavior. Further, Lacayo et al. [40] created an FE model of the Sumali beam and tuned the modal Iwan models such that their FE simulations closely matched the dynamic response measured by Deaner et al. In this work, the modal Iwan model identified in [40] for the second bending mode of the Sumali beam (shown in Fig. 2b) is taken as the truth model. It must be noted that the modal Iwan models in [6] were fit to match the amplitude-dependent resonant frequency and damping specifically in the microslip regime. One significant drawback of the Iwan model is the abrupt change in stiffness from the microslip to macroslip regime, a behavior that is not physically accurate. However, the model's ability to capture the power-law damping behavior accurately makes it a useful basis for comparison in this particular case study.

Table 1 lists the parameters of the modal Iwan model that best fits the second bending mode of the Sumali beam. These parameters result in a low-amplitude linear frequency of 213.94 Hz, and a macroslip frequency of 205.86 Hz. It was shown in [6] and [40] that the resulting amplitude-dependent frequency and damping curves produced by the modal Iwan model closely match experimental measurements. Therefore, the modal Iwan model can be considered to be the truth model for this system. While the Sumali beam tends to have lower damping than other jointed structures [41], it was chosen as a case study in this work because the behavior is still typical and its modal behavior has been thoroughly studied through both simulation and experiments. Following the comparative study with the Iwan model, the range of nonlinear behavior that a Bouc-Wen model can capture is also evaluated, allowing some generalization to other structures.

3.1 Procedure for Comparison Between the Hysteretic Models

First, an equivalent Bouc-Wen model must be identified using the method of least squares, outlined in Sec. 2.3. To do so, the force-displacement relationship of the modal Iwan model was estimated by performing a quasi-static analysis. The equation for the Iwan model under static loading reduces to

Table 1: Parameters of the four-parameter modal Iwan model that fits Mode 8 of the Sumali beam

Parameter	Value
(K_∞) [s^{-2}]	1.67×10^6
low-amplitude damping (ξ_0)	1×10^{-4}
F_s [N kg$^{-1/2}$]	1.518
(K_T) [s^{-2}]	1.34×10^5
χ	-0.162
β	2.000

$$K_\infty q + F_{\text{nl,Iwan}}(q, \phi) = F_{\text{static}}, \tag{12}$$

where q is the displacement of the mode under consideration, i.e. the second bending mode of the Sumali beam in the case presented. The above equation is nonlinear in nature and can be converted to the form $f(q) = 0$ by moving the term F_{static} to the left-hand side. Therefore, the displacement of the modal Iwan model, q, at a particular static force can be obtained by using the Newton-Raphson method to solve Eq. 12. This was done over a range of monotonically increasing static force amplitudes, up to a maximum value of $F_{\max}$, to generate the force-displacement backbone curve. Since the Iwan model is a Masing model, Masing's rules could be applied to estimate the complete hysteresis loop at the maximum force amplitude [42]. Note that, alternatively, one could use the Newton-Raphson method to estimate the complete hysteresis loop by applying static loads that result in loading, unloading and then reloading of the system. However, application of Masing's rules gives a quicker and equally accurate result. Once the complete force-displacement hysteresis loop was calculated, the method described in Sec. 2.3 was used to estimate the equivalent Bouc-Wen model parameters.

The resultant Bouc-Wen model was first statically excited to verify the least squares solution. The Bouc-Wen static formulation can be written as

$$K_\infty q + (1 - \alpha) K_0 z - F_{\text{static}} = 0 \tag{13}$$

where the hysteretic variable, z, is calculated by solving Eq. 4. Note, again, that the externally applied static force

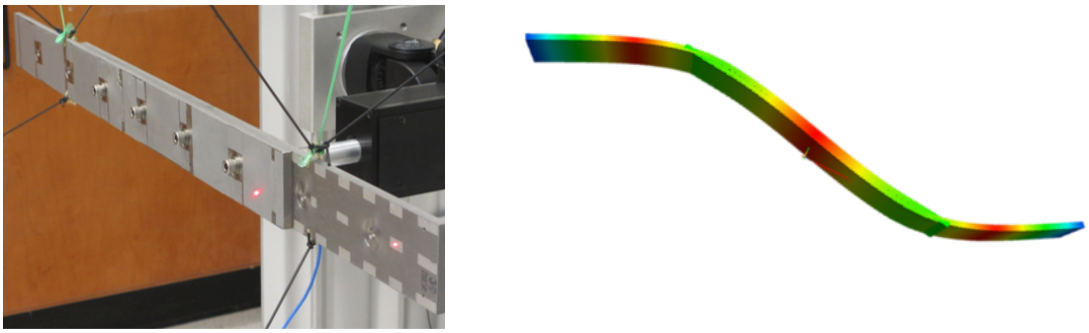

(a) (b)

Fig. 2: (a) Photograph of the Sumali beam structure and (b) Elastic Mode 8, the second bending mode

is written on the left-hand side for the equation to be of the form $f(q) = 0$. To solve Eq. 13 using the Newton-Raphson method, the modal displacement q was defined as a function of z. To do so, first, Eq. 4 can be rearranged as

$$\dot{z} = \dot{q}(1 - |z|^n(\text{sgn}(\dot{q}z)\beta + \gamma)). \tag{14}$$

The time dependence in Eq. 14 can be eliminated, resulting in Eq. 15.

$$dq = \frac{dz}{(1 - |z|^n(\text{sgn}(\dot{q}z)\beta + \gamma))} \tag{15}$$

The integral of the above equation is given by Gauss' hypergeometric function, ${}_2F_1(a, b; c; z)$, as shown in [34]. Therefore,

$$q = q_0 + z\,{}_2F_1\left(1, \frac{1}{n}; 1 + \frac{1}{n}; (\text{sgn}(\dot{q}z)\beta + \gamma)|z|^n\right)\Big|_{z_0}^{z} \tag{16}$$

Substituting Eq. 16 in Eq. 13 results in a nonlinear equation of the form $f(z) = 0$, which can be solved for z using the Newton-Raphson iteration method. Equation 16 can then be used to calculate the modal displacement at the force amplitude under consideration. The Bouc-Wen system was excited up to $F_{\max}$, the same maximum force amplitude as the Iwan model, followed by a decrease in the force to cause unloading up to $-F_{\max}$, and then an increase again to cause reloading up to $F_{\max}$. Thus, the complete hysteresis loop for the Bouc-Wen model was identified. Unlike the Iwan model, the Bouc-Wen model does not obey Masing's rules. Therefore, the complete cycle needs to be numerically simulated. Note that, alternatively, the Bouc-Wen response could have been numerically estimated by applying a harmonic force of low enough frequency such that the system can be approximated as being quasi-statically excited. The nonlinear EoM can then be solved using the Runge-Kutta method.

Once a Bouc-Wen model was obtained that could capture the steady-state hysteretic behavior, its ability to capture the amplitude-dependent system dynamics was evaluated. The response of the Bouc-Wen model to an impulsive force was simulated using the Runge-Kutta explicit ODE solver. On the other hand, the Newmark-β method was used to simulate the response of the Iwan model. In both cases, the impulsive force was modeled as one half of a sinusoid with a width of 0.005 s and the dynamic response was simulated for a time span of 10 s. Note that one dynamic analysis of the Iwan model using the Newmark-β method took 93.22 s, whereas the Runge-Kutta method for the Bouc-Wen model took 3.86 s. Both models were being simulated on an Intel(R) Core(TM) i7 CPU 950 @ 3.07GHz. This highlights the computational advantage offered by the Bouc-Wen model. The resulting time history in both cases was then post-processed using the Hilbert transform [43, 44] to compute the amplitude-dependent frequency and damping for comparison.

This analysis method was applied to three different cases comparing the Bouc-Wen model to the Iwan model. A description of the three cases and the results are discussed below.

3.2 Effect of the Parameter n on Dynamic Behavior

The parameter n in the Bouc-Wen model is known to determine the smoothness of the transition from microslip to macroslip [26]. When the parameter n tends to infinity, a bilinear model is obtained. According to existing

literature, the Bouc-Wen model is not sensitive to n [36] and in some applications, varying n does not significantly impact the results [31, 32]. The validity of this claim in case of bolted joints dynamics has been tested here.

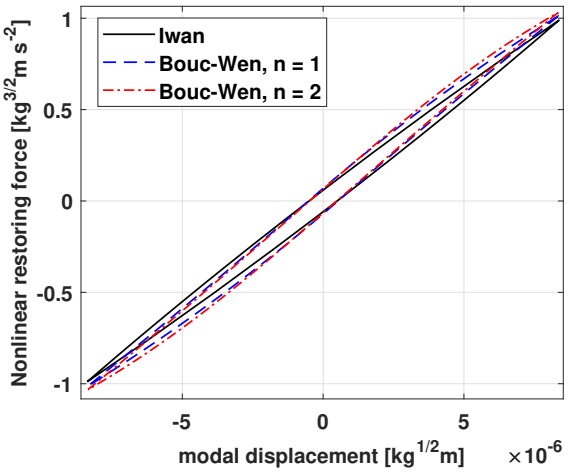

Fig. 3: Hysteresis curve when $n = 1$ (dashed line) and when $n = 2$ (dashed-dotted line) compared against the Iwan model (solid line)

Figure 3 shows the hysteresis loops calculated using the quasi-static analysis described in Sec. 3.1. The solid line is the estimate using the Iwan model, the dashed line is from the Bouc-Wen model with $n = 1$, and the dashed-dotted line is from the Bouc-Wen model with $n = 2$. It can be observed that the two values of n result in very similar steady-state behavior. The area inside the hysteresis loop for $n = 1$ equals 3.303×10^{-6} kg N m while that inside the hysteresis loop for $n = 2$ is nearly the same at 3.725×10^{-6} kg N m, giving a difference of $\approx 12\%$. However, the amplitude-dependent frequency and damping are of primary interest when characterizing bolted joint dynamics. Therefore, the effect of change in 'n' on the amplitude-dependent behavior was studied by applying an impulsive force, as described in Sec. 3.1. Figure 4 shows the frequency and damping, both plotted against the nondimensional velocity amplitude. Note that due to the nondimensionalization, the system is in macroslip when the X-coordinate equals 1. In the system presented, with $n = 1$ the Bouc-Wen model is able to match the true behavior (given by the Iwan model) more closely, with a maximum error of 0.17%. On the other hand, when $n = 2$, the frequency changes abruptly and the maximum error is 0.49%. Figure 4b plots the nonlinear damping as a function of response amplitude. Similar to frequency, the damping estimate when $n = 1$ closely matches the Iwan model, with a maximum error of 17.8% while $n = 2$ shows significant deviation, with a maximum error of 67.4%. Thus, n appears to influence the amplitude-dependent nonlinear dynamics of the system and must be accounted for when identifying the Bouc-Wen model parameters. In the following cases, the parameter identification process was performed over a range of n values and the parameter set resulting in lowest error in the least squares solution was chosen. It should be noted that while the comparison above may suggest that the parameter n changes the power-law exponent of the Bouc-Wen model, the results in Fig. 8, discussed later, show that this is not the case.

3.3 Effect of Forcing Amplitude on Parameter Identification

One difficulty in comparing hysteretic models is that, because the damping is a weak effect, almost any hysteretic model or even a linear model can reproduce a given vibration measurement at a fixed amplitude. However, if the model does not correctly capture the variation in damping with vibration amplitude, it will only be accurate at the amplitude at which the fit was performed. In order to evaluate this for the Bouc-Wen model, the excitation level of the quasi-static analysis that was used to estimate the model parameters, i.e. $F_{\max}$, was varied and a Bouc-Wen model was fit to the quasi-static hysteresis loop obtained for each force amplitude. To quantify the level of slip at these different force amplitudes, the amplitude ratio, AR, was defined as the ratio of the maximum displacement at the applied load to the displacement at which macroslip occurs (i.e. $\phi_{\max}$). By definition, $\mathrm{AR} = 1$ indicates the amplitude of the quasi-static load applied is sufficient to cause macroslip.

$$\mathrm{AR} = \frac{x_{\max}}{\phi_{\max}} \tag{17}$$

The Bouc-Wen parameters that best fit the hysteresis loop for the different values of AR were calculated. Then, an impulsive force, with amplitude small enough for the system to remain in microslip, was applied to each of these Bouc-Wen models and the Fast Fourier Transform, or FFT, of the dynamic response was calculated. Figure 5 shows that there is a range of AR, specifically $0.1 < \mathrm{AR} < 1$, for which the resultant Bouc-Wen model gives nearly identical response. If macroslip level data is being fit, i.e. when $\mathrm{AR} > 1$, the Bouc-Wen model

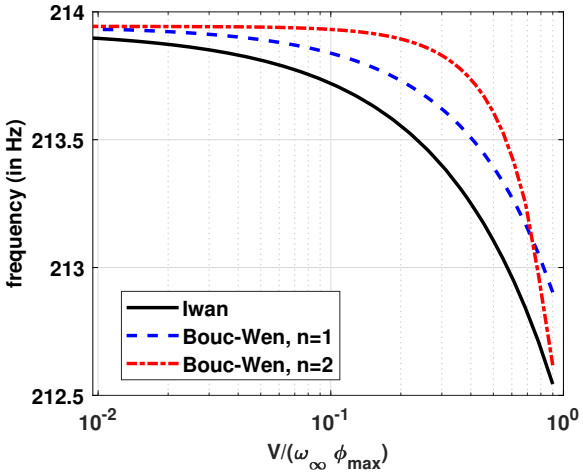

(a)

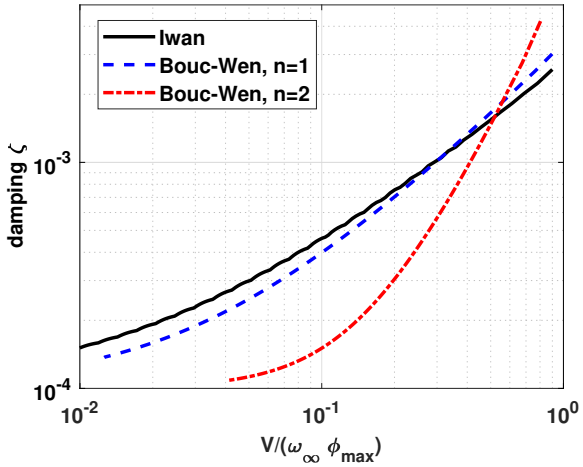

(b)

Fig. 4: Amplitude-dependent (a) frequency and (b) damping, for two different values of n, compared against the Iwan modal

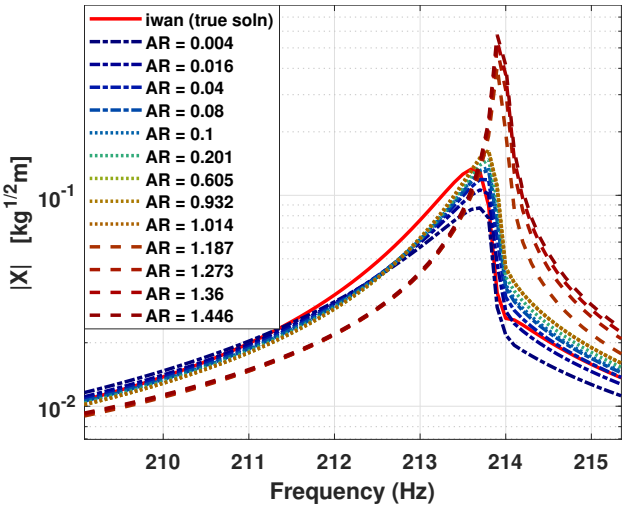

Fig. 5: FFT of the response to an impulsive force applied to the Bouc-Wen models obtained using forces that produce different values of the amplitude ratio (AR)

obtained is significantly different. This implies that two different Bouc-Wen models are required to simulate the behavior of an Iwan model.

The amplitude-dependent dynamic behavior was analyzed to further verify this claim. Two AR values were considered. For the first value, the model is in microslip (AR $= 0.4$) while for the second, it is in macroslip (AR $= 1.23$). An impulsive force large enough to capture both macroslip and microslip behavior was applied to both models and the resultant frequency and damping were calculated. As seen in Fig 6, the Bouc-Wen model obtained using AR $= 0.4$, shown using dashed lines, is able to estimate the frequency and damping in the microslip regime but is inaccurate in the macroslip regime. Note that a value of 1 on the X-axis corresponds to the onset of macroslip. On the other hand, the nonlinear dynamic behavior obtained using AR $= 1.23$, shown using dashed-dotted lines, is accurate in the macroslip region but not in microslip. This further proves that the same Bouc-Wen model cannot replicate both microslip as well as macroslip behavior of the Iwan model. Another observation of note here is that the Bouc-Wen model that best fits microslip data has $n = 1$, whereas the model that best fits macroslip data has $n \approx 5.5$. This also highlights the need to vary the parameter n, as discussed in Sec. 3.2. Table 2 lists the parameters of the Bouc-Wen model that best simulates the microslip-level behavior. Thus, this model results in the frequency and damping curves given by the dashed lines in Fig. 6.

3.4 Accuracy of the Bouc-Wen Model at Different Dissipation Levels

The parameter χ in the four-parameter Iwan model directly relates to the power-law behavior observed in the damping (or in the dissipation per cycle [19]). The slope of the damping vs amplitude, when plotted on a logarithmic scale, equals $1 + \chi$. (This corresponds to the energy dissipated per cycle having a slope of $3 + \chi$.) The value of χ typically varies between -1 and 0, with $\chi = -1$ corresponding to linear damping. In the prior case studies (i.e. in Sec. 3.2-3.3), $\chi = -0.162$ was used since it best captures the damping for mode 8 of the Sumali

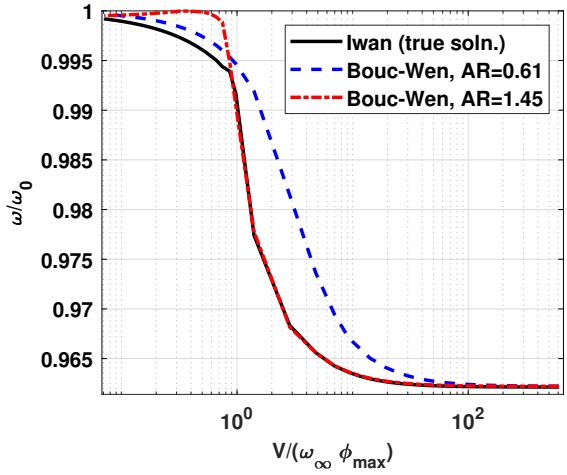

(a)

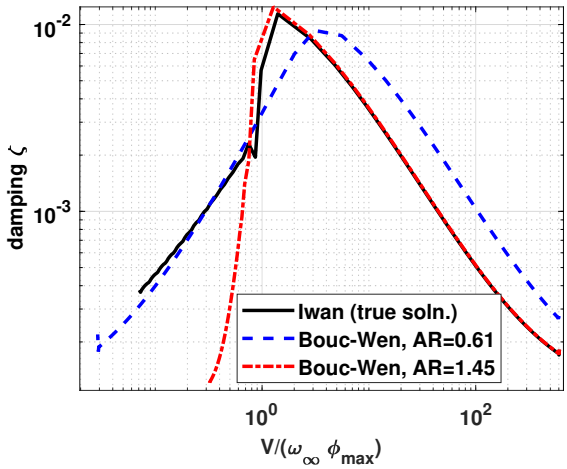

(b)

Fig. 6: Comparison of the nonlinear (a) frequency and, (b) damping when the AR used for fitting the Bouc-Wen model corresponds to microslip (dashed line) vs. macroslip (dashed-dotted line). The solid line is the result from the truth model.

beam. This corresponds to the damping curve having a slope of 0.838 in the microslip regime when plotted on the logarithmic scale, as shown by the solid line in Fig. 7a. The value of χ was then changed to $\chi = -0.6$ with the other parameters left constant, and the comparison repeated, with the results shown in Fig. 7b. As a result, the modal Iwan model used no longer matches measurements from mode 8 of the Sumali beam. However, such a value of χ is still within the range of damping behavior observed in other bolted structures. For example, χ values between -0.280 and -0.400 were observed in [7]. Comparing the results for the two cases, when $\chi = -0.162$, the Bouc-Wen model exhibits a similar trend to the Iwan model but underestimates the damping, with a maximum error of 18.1%. However, when χ is changed to -0.6, the Bouc-Wen model significantly deviates from the Iwan model, with a maximum error of 67.2%. Therefore, it appears that the Bouc-Wen model is less effective at capturing the modal behavior of a system when the power law behavior has a smaller slope.

Table 2: Parameters of the modal Bouc-Wen model that best fits microslip behavior of mode 8 of the Sumali beam (given by the four-parameter Iwan model in Tab. 1)

Parameter	Value
A	1
β	1.41×10^4
γ	2.32×10^4
n	1

Note that, for each value of χ, the Bouc-Wen model that best fit the quasi-static response of the Iwan model was estimated. Then, the response of both the Bouc-Wen and Iwan models to an impulsive force was calculated. In each case the quasi-static data used to identify the Bouc-Wen model corresponded to the microslip regime, and the amplitude of impulsive force applied when computing the dynamic response was also limited so that the response of the system remained in the microslip regime.

Figure 8 further compares the nonlinear damping as a function of amplitude for a range of χ values to better observe the damping trend followed by the Bouc-Wen model. The different colors correspond to different values of χ. For each color, the solid line is the damping for the Iwan model, and the dashed-dotted line of the same color is the damping for the best-fit Bouc-Wen model. Both axes have logarithmic scales so that the power-law behavior can be easily observed. As expected, the Iwan model gives straight lines of varying slopes for different χ values until the response amplitude is low enough for the linear damping to dominate. The slope of damping increases as the value of χ increases (note that χ assumes negative values). The Bouc-Wen model, on the other hand, exhibits little difference in the damping behavior, regardless of the value of χ of the system that one is trying to represent. The damping versus amplitude produced by the Bouc-Wen model is approximately straight line on the

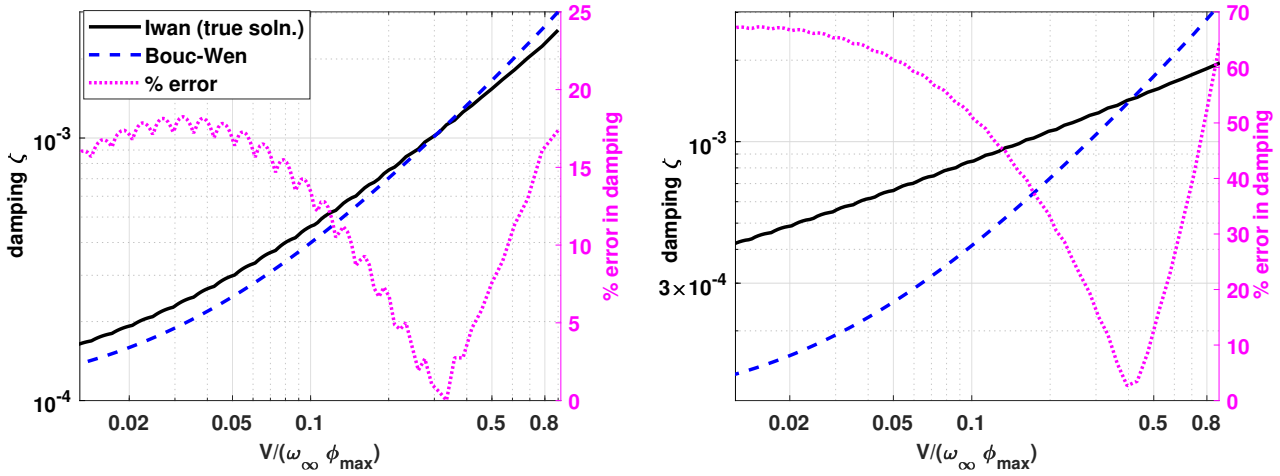

(a) $\chi = -0.162$ (b) $\chi = -0.6$

Fig. 7: Comparison of the damping estimated by the Bouc-Wen model against the Iwan model when (a) $\chi = -0.162$, and when (b) $\chi = -.6$ for the Iwan model. The left y-axis shows the damping and the right y-xis shows the error in damping, both plotted against the non-dimensional velocity on the x-axis.

log-log plot, indicating that the Bouc-Wen model does exhibit power-law behavior, but the slope of the line varies little. For lower values of χ, the equivalent Bouc-Wen model shows significant deviation from the Iwan model damping curve. However, for higher χ values, for example when $\chi = -0.01$, the damping estimated by the Bouc-Wen model closely matches the Iwan model. This indicates that the Bouc-Wen model is more suitable when the power law slope is closer to 1 or when $\chi \approx 0$.

3.5 Discussion

The comparisons presented here take the true behavior to be that of an Iwan model that has been tuned to match the behavior of a single mode of the Sumali beam. The results have shown that the Bouc-Wen model is limited in its ability to capture this behavior. This is important because the power-law damping behavior captured by the Iwan element is a feature of important analytical models such as the Mindlin solution [19] and many structures have been shown to exhibit Iwan-like behavior [5–7]. However, there are certainly many systems that behave differently; in those cases one might find that the Bouc-Wen model is more faithful in reproducing the desired behavior. Additionally, the Bouc-Wen model may be more capable of reproducing the behavior of an Iwan element if different parameters were chosen for the latter. The next section explores the capabilities of the Bouc-Wen model in more general terms, showing how each term affects its damping versus amplitude behavior.

4 EFFECT OF EACH BOUC-WEN PARAMETER ON THE DAMPING

In the different case studies considered above, all the parameters of the Bouc-Wen model were allowed to vary such that the resultant set best fit the Iwan model behavior. This section studies the effect of changing a single parameter at a time on the damping behavior of the Bouc-Wen model. To do so, the Bouc-Wen parameters that best fit the Iwan model for mode 8 of the Sumali beam were considered as a starting point. First, the parameter β was varied from 0.8×10^4 to 1.5×10^5, increasing by nearly 20 times over the range. Note that the value of β for the Sumali beam model was 1.41×10^4 (as shown in Tab. 2), thus lying within the range considered here. An impulsive force was applied to the resulting Bouc-Wen model for all values of β, and the time history was post-processed using the Hilbert transform to estimate the amplitude-dependent damping. Figure 9a shows the damping for the different values of β. It can be seen that increasing β results in the damping curve shifting upwards, along the Y-axis. This means that for the same response amplitude, a higher β results in a higher damping (or dissipation of energy). However, the slope of the curve itself shows negligible change.

Next, the Bouc-Wen parameter γ was varied, with all other parameters corresponding to the model that best fit mode 8 of the Sumali Beam, as in the previous sections. The original value of γ was 2.32×10^4. Thus, it was varied from 1×10^4 to 1×10^6, a hundredfold increase over

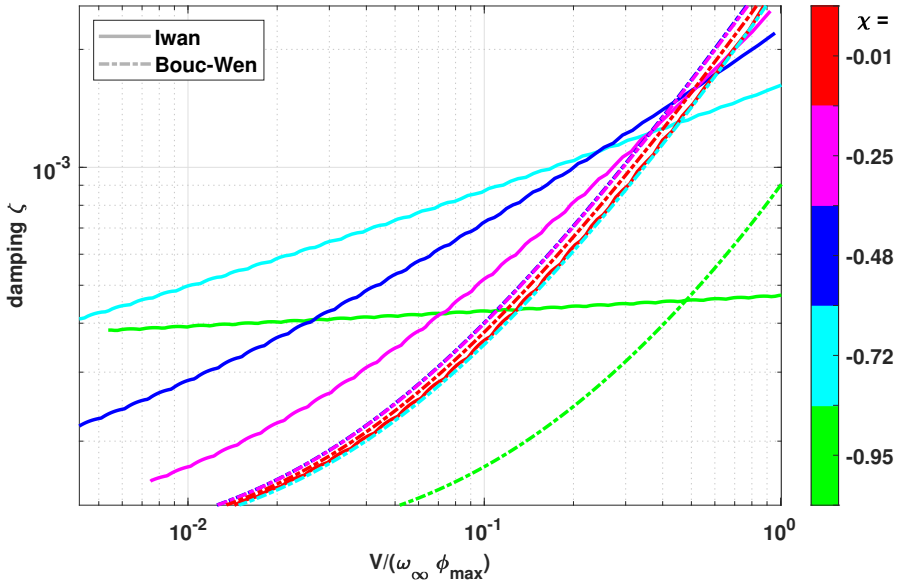

Fig. 8: Comparison of the damping estimated by the Bouc-Wen model against the Iwan model for different values of the Iwan model parameter χ. This parameter changes the slope of the damping vs. response amplitude curve, when plotted on a logarithmic scale. The solid lines correspond to the Iwan model and the dashed-dotted lines represent the Bouc-Wen model estimate. The different colors correspond to different values of χ between -1 and 0. (Refer to the online version of this article to interpret references to color in this figure.)

the range. The nonlinear damping for all values of γ was estimated using the response to an impulsive force, with the results plotted in Fig. 9b. At low response amplitudes, the damping curves show negligible difference. However, as the amplitude increases and approaches macroslip, the curves diverge. Note that macroslip is the point at which the damping is the highest. As γ increases, the point at which macroslip occurs shifts to the left along the X-axis, i.e. to a lower response amplitude. Therefore, the parameter γ impacts the damping behavior of the Bouc-Wen model only near macroslip; the lower-amplitude microslip behavior is largely unaffected.

Finally, the parameter n, that appears as an exponent in the differential equation defining the Bouc-Wen model, was varied. Note that in Sec. 3.2, for each value of n considered, all the Bouc-Wen parameters were updated to obtain the best fit to a mode with a certain damping versus amplitude curve. Here, however, only n was varied, setting all other parameters to the values in Tab. 2. Figure 10 shows the resultant amplitude-dependent damping for $1 \leq n \leq 2$. Increasing n results in the damping curve shifting horizontally towards the right. This means that for the same response amplitude, a higher value of n gives lower damping when the system is in microslip. The increase in n also results in a delay in macroslip, i.e. a larger amplitude is required to cause the system to go into macroslip. However, the slope of the damping curve in the microslip regime remains largely unaltered. Note that these trends were observed to continue for higher values of n. A smaller range was chosen here for clear visualization and easy interpretation.

Considering all of the results in this study, it can be concluded that, while the Bouc-Wen model does exhibit power-law dissipation behavior, the slope of that behavior is roughly fixed and corresponds to that of an Iwan model with $\chi \approx 0$; the log damping versus log amplitude curve has a slope of $+1$. None of the parameters of the Bouc-Wen model are effective in varying that slope over a large amplitude range. If capturing steady-state response is of interest, or the system is expected to operate over a small amplitude range, the Bouc-Wen model could still be used. For example, Fantetti et al. [31] developed a wear-dependent Bouc-Wen model that successfully captured the impact of long-term wear on the steady-state behavior of frictional contact. Similarly, the Bouc-Wen model has been successfully used to simulate the hysteretic behavior of magnetorheological dampers [45] as well as concrete structural elements [46]. It must be noted that these appli-

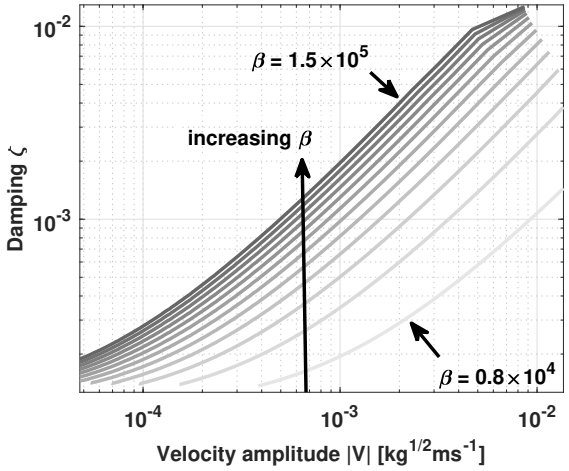

(a)

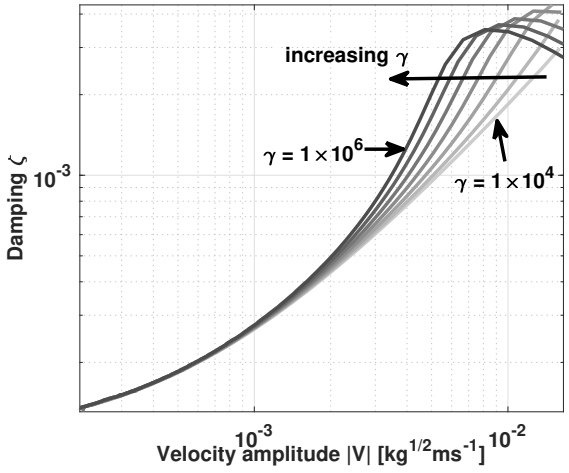

(b)

Fig. 9: Effect of varying the Bouc-Wen parameters (a) β, and (b) γ on the amplitude-dependent damping

cations, apart from focusing on steady-state dynamics, involve modeling of complete slip behavior. Alternatively, a parallel arrangement of Bouc-Wen models with varying parameters could potentially be designed to capture the nonlinear behavior over a large amplitude range. However, this method requires further investigation.

5 CONCLUSIONS

This paper explored the ability of the Bouc-Wen model to capture the power-law damping behavior that is characteristic of structures with bolted joints. Three important observations were made when comparing the

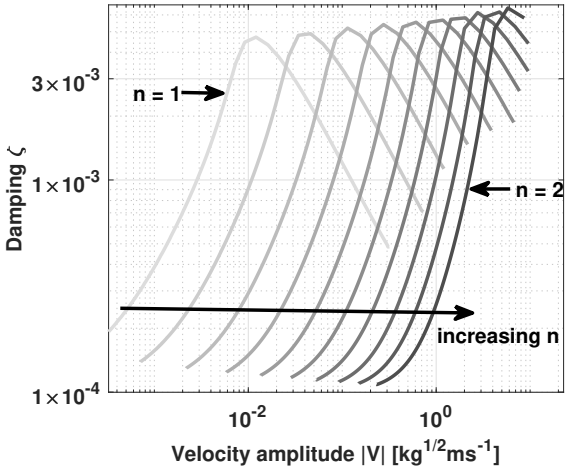

Fig. 10: Effect of varying the Bouc-Wen parameter n on the amplitude-dependent damping

Bouc-Wen model to the four-parameter Iwan model. First, it was observed that the value of the Bouc-Wen parameter n has a significant effect on the amplitude-dependent frequency and damping estimated by the model. While existing literature shows that the hysteresis loop itself is not sensitive to small changes in n, this paper shows that n needs to be varied for the Bouc-Wen model to better estimate the dynamic behavior of a system over a range of amplitudes. The second observation was that a single Bouc-Wen model cannot simulate both microslip and macroslip level nonlinearity. The parameters can be adjusted to capture either microslip or macroslip, but not both simultaneously. This also must be considered when identifying the Bouc-Wen model parameters from quasi-static responses. For low amplitude ratios, when the system is in microslip, similar Bouc-Wen model parameters were obtained regardless of the amplitude of quasi-static excitation used to identify the system. However, once the system goes into macroslip, a different set of parameters are required to correctly fit the hysteretic behavior. Thirdly, the effect of changing the parameter χ, that defines slope of the log damping versus log of the vibration amplitude, was studied. A lower value of χ corresponds to the dissipation versus amplitude curve having a lower slope, when plotted in the logarithmic scale. The Bouc-Wen model was observed to have a power-law slope of $\approx +1$ (corresponding to $\chi \approx 0$). When the system of interest had a smaller power-law slope, the Bouc-Wen model became increasingly inaccurate. Hence, while the Bouc-Wen model is conceptually simple and computationally efficient, it is limited in the range of microslip-

level dynamic behavior that it can simulate.

The effect of each Bouc-Wen parameter on the overall damping was also studied. It was found that increasing the parameter β causes the damping curve to shift vertically upwards, while increasing n results in a horizontal shift. However, the slope of the damping curve in the microslip regime does not change significantly in either case. On the other hand, the parameter γ changes the slope of the curve near macroslip, with the damping at lower-amplitudes remaining largely unaffected. Thus, none of the Bouc-Wen model parameters can capture the microslip-level power-law damping behavior over a large range of amplitudes that is known to be characteristic of bolted joints. However, one may be able to choose parameters that adequately capture the average damping over a small enough range of force amplitudes, and in those cases the Bouc-Wen model can still be extremely useful. In the future, it would be interesting to explore whether a parallel arrangement of Bouc-Wen models can be tuned to capture power-law behavior over a wider range of amplitudes, while still retaining reasonable computational efficiency.

REFERENCES

[1] Richards, E. J., and Mead, D. J., 1968, *Noise and Acoustic Fatigue in Aeronautics*, 1st edition ed. Chichester, United Kingdom: John Wiley & Sons Ltd, London New York Sydney Toronto.

[2] Ungar, E., 1973, "The Status of Engineering Knowledge Concerning the Damping of Built-up Structures," *Journal of Sound and Vibration,* **26**(1), pp. 141–154.

[3] Gaul, L., and Lenz, J., 1997, "Nonlinear Dynamics of Structures Assembled by Bolted Joints," *Acta Mechanica,* **125**(1), pp. 169–181.

[4] Lenz, J., and Gaul, L., 1995, "The Influence of Microslip on the Dynamic Behavior of Bolted Joints," In Proceedings of the International Modal Analysis Conference (IMAC XXIII), pp. 248–254.

[5] Smallwood, D. O., Gregory, D. L., and Coleman, R. G., 2000, Damping Investigations of a Simplified Frictional Shear Joint Tech. Rep. SAND2000-1929C, Sandia National Lab. (SNL-NM), Albuquerque, NM (US);Sandia National Labs., Livermore, CA (US).

[6] Deaner, B. J., Allen, M. S., Starr, M. J., Segalman, D. J., and Sumali, H., 2015, "Application of Viscous and Iwan Modal Damping Models to Experimental Measurements From Bolted Structures," *Journal of Vibration and Acoustics,* **137**(2), p. 021012.

[7] Roettgen, D. R., and Allen, M. S., 2017, "Nonlinear Characterization of a Bolted, Industrial Structure Using a Modal Framework," *Mechanical Systems and Signal Processing,* **84**, pp. 152 – 170.

[8] Goodman, L. E., 1980, "Contributions of continuum mechanics to the analysis of the sliding of unlubricated solids," In AMD Symposium Series of the ASME Applied Mechanics Division, Vol. 39, pp. 1–12.

[9] Segalman, D. J., 2006, "Modelling Joint Friction in Structural Dynamics," *Structural Control and Health Monitoring,* **13**(1), pp. 430–453.

[10] Lee, S.-Y., Ko, K.-H., and Lee, J. M., 2000, "Analysis of Dynamic Characteristics of Structural Joints Using Stiffness Influence Coefficients," *Journal of Mechanical Science and Technology,* **12**(14), pp. 1319–1327.

[11] Jewell, E., Allen, M. S., Zare, I., and Wall, M., 2020, "Application of quasi-static modal analysis to a finite element model and experimental correlation," *Journal of Sound and Vibration,* **479**, Aug., p. 115376.

[12] Segalman, D. J., 2001, An Initial Overview of Iwan Modeling for Mechanical Joints Tech. Rep. SAND2001-0811, 780307, Sandia National Lab. (SNL-NM), Albuquerque, NM (United States), Mar.

[13] Najera-Flores, D. A., and Kuether, R. J., 2020, "A Study of Whole Joint Model Calibration Using Quasi-Static Modal Analysis," *Journal of Vibration and Acoustics,* **142**(5), June.

[14] Segalman, D. J., 2010, A Modal Approach to Modeling Spatially Distributed Vibration Energy Dissipation. Tech. Rep. SAND2010-4763, 993326, Sandia National Lab., Albuquerque, NM.

[15] Gaul, L., and Nitsche, R., 2001, "The Role of Friction in Mechanical Joints," *Applied Mechanics Reviews,* **54**(2), Mar., pp. 93–106.

[16] Mathis, A. T., Balaji, N. N., Kuether, R. J., Brink, A. R., Brake, M. R. W., and Quinn, D. D., 2020, "A Review of Damping Models for Structures With Mechanical Joints1," *Applied Mechanics Reviews,* **72**(4), July, p. 040802.

[17] Iwan, W. D., 1966, "A Distributed-Element Model for Hysteresis and Its Steady-State Dynamic Response," *Journal of Applied Mechanics,* **33**(4), Dec., pp. 893–900.

[18] Song, Y., Hartwigsen, C. J., McFarland, D. M., Vakakis, A. F., and Bergman, L. A., 2004, "Simulation of dynamics of beam structures with bolted joints using adjusted Iwan beam elements," *Journal of Sound and Vibration,* **273**(1), May, pp. 249–276.

[19] Segalman, D. J., 2005, "A Four-Parameter Iwan Model for Lap-Type Joints," *Journal of Applied Me-*

chanics, **72**(5).

[20] Mignolet, M. P., Song, P., and Wang, X. Q., 2015, "A Stochastic Iwan-Type Model for Joint Behavior Variability Modeling," *Journal of Sound and Vibration,* **349**, Aug., pp. 289–298.

[21] Brake, M. R. W., 2017, "A Reduced Iwan Model That Includes Pinning for Bolted Joint Mechanics," *Nonlinear Dynamics,* **87**(2), pp. 1335–1349.

[22] Shetty, D., and Allen, M., 2020, "Fast Simulation of a Single Degree-of-Freedom System Consisting of An Iwan Element Using the Method of Averaging," *Journal of Vibration and Acoustics,* **142**(5), Oct., p. 051107.

[23] Bouc, R., 1971, "A Mathematical Model for Hysteresis," *Acustica,* **21**, pp. 16–25.

[24] Wen, Y.-K., 1976, "Method for Random Vibration of Hysteretic Systems," *Journal of the Engineering Mechanics Division,* **102**(2), pp. 249–263 Publisher: ASCE.

[25] Dormand, J. R., and Prince, P. J., 1980, "A family of embedded Runge-Kutta formulae," *Journal of Computational and Applied Mathematics,* **6**(1), Mar., pp. 19–26.

[26] Ismail, M., Ikhouane, F., and Rodellar, J., 2009, "The Hysteresis Bouc-Wen Model, a Survey," *Archives of Computational Methods in Engineering,* **16**(2), June, pp. 161–188.

[27] Low, T. S., and Guo, W., 1995, "Modeling of a Three-Layer Piezoelectric Bimorph Beam with Hysteresis," *Journal of Microelectromechanical Systems,* **4**(4), Dec., pp. 230–237 Conference Name: Journal of Microelectromechanical Systems.

[28] Yoshioka, H., Ramallo, J. C., and Spencer, B. F., 2002, ""Smart" Base Isolation Strategies Employing Magnetorheological Dampers," *Journal of Engineering Mechanics,* **128**(5), May, pp. 540–551 Publisher: American Society of Civil Engineers.

[29] Foliente, G. C., 1995, "Hysteresis Modeling of Wood Joints and Structural Systems," *Journal of Structural Engineering,* **121**(6), June, pp. 1013–1022 Publisher: American Society of Civil Engineers.

[30] Oldfield, M., Ouyang, H., and Mottershead, J. E., 2005, "Simplified Models of Bolted Joints Under Harmonic Loading," *Computers & Structures,* **84**(1), Dec., pp. 25–33.

[31] Fantetti, A., Tamatam, L. R., Volvert, M., Lawal, I., Liu, L., Salles, L., Brake, M. R. W., Schwingshackl, C. W., and Nowell, D., 2019, "The Impact of Fretting Wear on Structural Dynamics: Experiment and Simulation," *Tribology International,* **138**, Oct., pp. 111–124.

[32] Allen, M. S., Schoneman, J., Scott, W., and Sills, J., 2021, "Application of Quasi-Static Modal Analysis to an Orion Multi-Purpose Crew Vehicle Test," In Sensors and Instrumentation, Aircraft/Aerospace, Energy Harvesting & Dynamic Environments Testing, Volume 7, C. Walber, P. Walter, and S. Seidlitz, eds., Conference Proceedings of the Society for Experimental Mechanics Series, Springer International Publishing, pp. 65–75.

[33] Porter, J. H., Balaji, N. N., Little, C. R., and Brake, M. R. W., 2022, "A quantitative assessment of the model form error of friction models across different interface representations for jointed structures," *Mechanical Systems and Signal Processing,* **163**, Jan., p. 108163.

[34] Charalampakis, A. E., and Koumousis, V. K., 2008, "On the response and dissipated energy of Bouc–Wen hysteretic model," *Journal of Sound and Vibration,* **309**(3), Jan., pp. 887–895.

[35] Guo, K., Zhang, X., Li, H., Hua, H., and Meng, G., 2008, "A New Dynamical Friction Model," *International Journal of Modern Physics B,* **22**(08), Mar., pp. 967–980 Publisher: World Scientific Publishing Co.

[36] Zhu, X., and Lu, X., 2011, "Parametric Identification of Bouc-Wen Model and Its Application in Mild Steel Damper Modeling," *Procedia Engineering,* **14**, pp. 318–324.

[37] Eriten, M., Kurt, M., Luo, G., Michael McFarland, D., Bergman, L. A., and Vakakis, A. F., 2013, "Nonlinear system identification of frictional effects in a beam with a bolted joint connection," *Mechanical Systems and Signal Processing,* **39**(1), Aug., pp. 245–264.

[38] Moldenhauer, B. J., Singh, A., Thoenen, P., Roettgen, D. R., Pacini, B. R., Kuether, R. J., and Allen, M. S., 2020, "Influences of Modal Coupling on Experimentally Extracted Nonlinear Modal Models," In Nonlinear Structures and Systems, Volume 1, G. Kerschen, M. R. W. Brake, and L. Renson, eds., Conference Proceedings of the Society for Experimental Mechanics Series, Springer International Publishing, pp. 189–204.

[39] Wall, M., Allen, M. S., and Kuether, R. J., 2022, "Observations of modal coupling due to bolted joints in an experimental benchmark structure," *Mechanical Systems and Signal Processing,* **162**, Jan., p. 107968.

[40] Lacayo, R. M., Deaner, B. J., and Allen, M. S., 2017, "A Numerical Study on the Limitations of Modal Iwan Models for Impulsive Excitations," *Journal of Sound and Vibration,* **390**, pp. 118–140.

[41] Brake, M. R., ed., 2018, *The Mechanics of Jointed Structures* Springer International Publishing, Cham.

[42] Jayakumar, P., 1987, "Modeling and identification in structural dynamics," Report or Paper, California Institute of Technology, Pasadena, CA, May Issue: 87-01 Number: 87-01 Publisher: California Institute of Technology.

[43] Feldman, M., 1994, "Non-Linear System Vibration Analysis Using Hilbert Transform–I. Free Vibration Analysis Method 'Freevib'," *Mechanical Systems and Signal Processing,* **8**(2), Mar., pp. 119–127.

[44] Sumali, H., and Kellogg, R. A., 2011, Calculating Damping from Ring-Down Using Hilbert Transform and Curve Fitting. Tech. Rep. SAND2011-1960C, Sandia National Lab., Albuquerque, NM.

[45] Miah, M. S., Chatzi, E. N., Dertimanis, V. K., and Weber, F., 2015, "Nonlinear modeling of a rotational MR damper via an enhanced Bouc–Wen model," *Smart Materials and Structures,* **24**(10), Sept., p. 105020 Publisher: IOP Publishing.

[46] Pelliciari, M., Briseghella, B., Tondolo, F., Veneziano, L., Nuti, C., Greco, R., Lavorato, D., and Tarantino, A. M., 2020, "A degrading Bouc–Wen model for the hysteresis of reinforced concrete structural elements," *Structure and Infrastructure Engineering,* **16**(7), July, pp. 917–930 Publisher: Taylor & Francis _eprint: https://doi.org/10.1080/15732479.2019.1674893.